J Nonlinear Sci (2008) 18: 593–614
DOI 10.1007/s00332-008-9031-0

Journal of
Nonlinear
Science

A Mathematical Model of Intermittent Androgen Suppression for Prostate Cancer

Aiko Miyamura Ideta · Gouhei Tanaka · Takumi Takeuchi · Kazuyuki Aihara

Received: 15 May 2006 / Accepted: 4 September 2007 / Published online: 19 October 2008
© Springer Science+Business Media, LLC 2008

Abstract For several decades, androgen suppression has been the principal modality for treatment of advanced prostate cancer. Although the androgen deprivation is initially effective, most patients experience a relapse within several years due to the proliferation of so-called androgen-independent tumor cells. Bruchovsky et al. suggested in animal models that intermittent androgen suppression (IAS) can prolong the time to relapse when compared with continuous androgen suppression (CAS). Therefore, IAS has been expected to enhance clinical efficacy in conjunction with reduction in adverse effects and improvement in quality of life of patients during off-treatment periods. This paper presents a mathematical model that describes the growth of a prostate tumor under IAS therapy based on monitoring of the serum prostate-specific antigen (PSA). By treating the cancer tumor as a mixed assembly of androgen-dependent and androgen-independent cells, we investigate the difference between CAS and IAS with respect to factors affecting an androgen-independent relapse. Numerical and bifurcation analyses show how the tumor growth and the relapse time are influenced by the net growth rate of the androgen-independent cells, a protocol of the IAS therapy, and the mutation rate from androgen-dependent cells to androgen-independent ones.

A.M. Ideta · K. Aihara (✉)
ERATO Aihara Complexity Modelling Project, JST, Tokyo 153-8505, Japan
e-mail: aihara@sat.t.u-tokyo.ac.jp

G. Tanaka · K. Aihara
Institute of Industrial Science, University of Tokyo, Tokyo 153-8505, Japan

T. Takeuchi
Department of Urology, University of Tokyo, Tokyo 113-8655, Japan

Keywords Prostate cancer · Intermittent androgen suppression · Mathematical modeling · Hybrid systems · Hysteresis · Bifurcations

Mathematics Subject Classification (2000) 34C55 · 37G15 · 65L07 · 92C50 · 93A30

Abbreviations

AD: androgen-dependent;
ADT: androgen deprivation therapy;
AI: androgen-independent;
CAS: continuous androgen suppression;
IAS: intermittent androgen suppression;
LHRH: luteinizing hormone releasing hormone;
MAB: maximal androgen blockade;
PSA: prostate-specific antigen.

1 Introduction

The prostate gland produces and secretes seminal fluid. Nevertheless, the essential functions of the prostate are still controversial. If cancer cells are detected in the prostate gland, the patient is diagnosed as the adenocarcinoma of the prostate. The screening of prostate cancer is currently conducted by using the serum prostate-specific antigen (PSA) test together with other methods like imaging and digital rectal examination. The PSA is a good biomarker for early detection of prostate cancer as well as estimation of its progress. One of the major treatments for advanced or metastatic prostate cancer is hormonal therapy; this is often combined with surgical, chemical, and radiation modalities depending on the stage of the cancer. At present, the cause of prostate cancer is not fully understood and its effective prevention has not been established; however, genes, lifestyle-related factors (Nelson et al. 2003), and aging are regarded as influential factors.

For a long time, it has been known that prostate cancer growth is stimulated by androgens, or male sexual hormones that are secreted by organs such as the testicles and the adrenal glands. Androgens circulate in the blood and diffuse into the tissue where they stimulate the prostate tumor to grow. Huggins and Hodges (1941) demonstrated the benefits of the ablation of testicular functions by orchiectomy, or surgical removal of the testes. Ever since, androgen deprivation therapy (ADT) has been the important treatment of advanced prostate cancer. Androgen deprivation can also be achieved by chemical castration, which is by administration of pharmacological agents such as luteinizing hormone releasing hormone (LHRH) analogs that inhibit the production of androgens from its primary source or the testes. The influence of the remaining androgens that are produced by other sources such as the adrenal glands can be eliminated by additional treatment with androgen-receptor antagonists (antiandrogens). The combination of antiandrogens with surgical/medical castration is known as maximal androgen blockade (MAB). Both ADT and MAB can facilitate apoptosis, or programmed death of androgen-dependent (AD) cancer cells, and quickly induce temporal regression of tumors (Bladou et al. 1996;

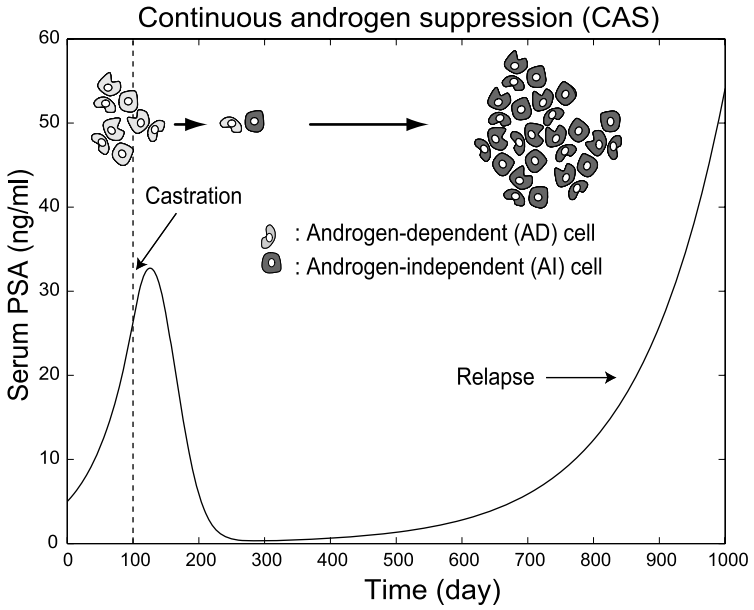

Fig. 1 Schematic illustration of tumor growth under CAS therapy for prostate cancer. Although the AD cells are drastically reduced immediately after the initiation of CAS, a PSA relapse often occurs within several years due to the growth of AI cells

Feldman and Feldman 2001; Scher et al. 2004; Dehm and Tindall 2005). However, most patients undergo a relapse with an increase of the serum PSA level within several years after the initiation of hormonal therapy (Feldman and Feldman 2001; McLeod 2003; Scher et al. 2004; Dehm and Tindall 2005; Edwards and Bartlett 2005). The so-called androgen-independent (AI) cells are considered to be responsible for this recurrent tumor growth. These cells are not sensitive to androgen suppression but rather apt to increase even in an androgen-depleted environment (Feldman and Feldman 2001; McLeod 2003; Scher et al. 2004; Dehm and Tindall 2005; Edwards and Bartlett 2005; Bruchovsky et al. 1990, 1996; Akakura et al. 1993). Once the tumor acquires androgen independence or hormone refractoriness, in which the androgen suppression no longer has a regressive effect on the tumor, the androgen deprivation would be unable to inhibit the cancer growth; an eventual tumor relapse is therefore inevitable. Figure 1 schematically illustrates a typical tumor growth resulting in an AI relapse under continuous androgen suppression (CAS) therapy of ADT and MAB. In hormonal therapy, it is an important issue to prevent a relapse or delay the time to relapse as long as possible. At the same time, it is clinically significant to reduce economic costs and alleviate adverse effects of prolonged androgen suppression.

A possible strategy to delay the progression from the AD state to the AI state is intermittent androgen suppression (IAS), which is a form of androgen ablative therapy delivered intermittently with off-treatment periods (Bruchovsky et al. 1990, 1996, 2000, 2001, 2006, 2007; Akakura et al. 1993; Bhandari et al. 2005). Under successful IAS therapy, the cycles of growth and regression of a prostate tu-

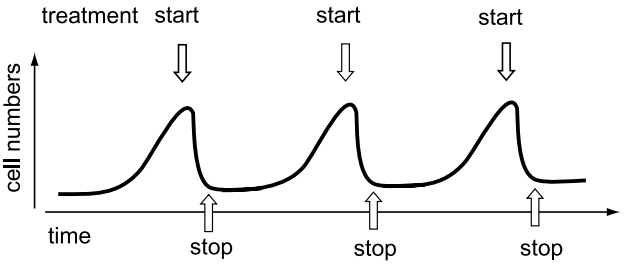

Fig. 2 Schematic illustration of the cycles of tumor growth and regression under IAS therapy. The introduction of off-treatment periods aims to prevent the tumor from becoming an androgen-refractory state in which androgen deprivation cannot evoke the apoptotic ability of the malignant cells and induce the regression of the tumor anymore

mor can be expected to remain under appropriate control of administration, as shown in Fig. 2. In order to avoid the emergence of AI cells due to androgen depletion, the IAS therapy introduces off-treatment terms that serve to maintain the androgen-deprivation sensitivity of the cancer cells and restore their apoptotic potential which can be induced by androgen deprivation. While the clinical efficacy of the IAS therapy was suggested in animal models (Bruchovsky et al. 1990; Akakura et al. 1993), a series of phase II studies on IAS demonstrated its potential and provided the clinical data beneficial for the intermittent administration (Bruchovsky et al. 2000, 2001, 2006, 2007; Bhandari et al. 2005). Most studies have confirmed improvement in the quality of life during the off-treatment periods and alleviation of adverse reactions such as hot flushes, sexual dysfunction, and osteoporosis. The clinical examples of the IAS therapy, including the phase II and ongoing phase III trials, are summarized in the review article (Bhandari et al. 2005). However, it remains unknown how to optimally plan the IAS therapy, i.e., when to discontinue and reinstitute the administration for androgen suppression, while monitoring the time course of the serum PSA level. Thus, the potential to practically use IAS, in comparison with CAS, must be further validated. This is the main problem to be considered in this paper.

The effect of CAS on the treatment of prostate cancer has been studied with a mathematical model based on experimental observations in order to understand biological characteristics of prostate tumors (Jackson 2004a, 2004b). The previous study intended to examine the progression to androgen independence and the resulting AI relapse during CAS by describing a tumor as an assembly of AD and AI cells. It was assumed that an AI relapse of a tumor could possibly result from the post-therapy decrease in the apoptotic rate of the AI cells. In this model, prostate tumor growth is described with the proliferation and apoptotic death rates of tumor cells. The model well reproduced the three phases of the prostate cancer progression, including the exponential growth prior to treatment, androgen-deprivation sensitivity immediately after the initiation of CAS therapy, and the eventual AI relapse of the tumor. Moreover, it was predicted that the CAS therapy is successful only for a small range of biological parameters.

In this paper, we propose a mathematical model that describes the prostate tumor growth under IAS therapy in order to compare with that under CAS therapy. Our

model is based on the formulation of the growth of a tumor consisting of AD and AI cells whose proliferation and apoptosis rates are dependent on the androgen concentration as in the former model (Jackson 2004a, 2004b). The main feature of our model lies in introduction of the IAS treatment and consideration of the mutational effect which is thought as one of the pathways leading to an AI relapse. The incorporation of the intermittent administration into the model leads to description of the model as a hybrid dynamical system (Johnson 1994; Guckenheimer and Johnson 1995; van der Schaft and Schumacher 2000; Savkin and Evans 2001) that switches dynamics between the on-treatment and the off-treatment periods because the androgen dynamics is completely different depending on presence or absence of the administration and the population dynamics of AD and AI cells is supposed to be influenced by the androgen concentration. The switching of the administration based on observation of the serum PSA level can be viewed as feedback control of the observable output of the system. As a result, the IAS therapy model generates richer dynamical behavior including periodic oscillations representing successful IAS therapy and even chaotic ones due to hysteresis, than the former model (Jackson 2004a, 2004b) for the CAS therapy does. The aim of IAS is to delay or preferably prevent an AI relapse by continuing the on-off cycles of administration. We show in the following that the net growth rate of the AI cells and the mutation rate largely affect the time to relapse and the parameter range for relapse prevention when the net growth rate of the AD cells is fixed at the physiologically plausible value. Further, bifurcation analysis of the hybrid dynamical system reveals the parameter conditions for occurrence and prevention of a relapse, which are characterized by divergent and nondivergent solutions, respectively. The results show that the IAS therapy enables to prevent a relapse with an appropriate protocol of the IAS treatment under biologically relevant assumptions. Based on the numerical results, the validity of the IAS therapy is further discussed. Throughout this paper, the fourth order Runge–Kutta method is used for the numerical integration of differential equations.

2 Formulation of Prostate Tumor Growth

2.1 Mathematical Descriptions

We first consider dynamics of the prostate tumor growth and the androgen concentration with and without administration for androgen suppression, as illustrated in Fig. 3. The administered dose is almost constant during on-treatment periods in the IAS therapy if the widely used androgen ablation therapy with the combination of LHRH analogs and antiandrogens, which is known as total androgen ablation or MAB (Feldman and Feldman 2001), is considered. Therefore, we assume that the administration is alternatively either present ($u = 1$) or absent ($u = 0$). If the administration is initiated in an androgen-rich condition, the androgen level drastically decays to almost zero. On the other hand, if the administration is suspended in an androgen-poor condition, the androgen level is recovered and assumed to be maintained at a nearly normal state. Considering these two responses, we describe the

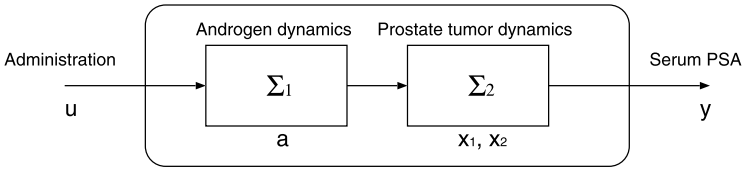

Fig. 3 Block diagram representing the tumor growth with and without hormonal therapy. The androgen dynamics depending on the presence or absence of administration influences the prostate tumor dynamics. The monitored biomarker is the serum PSA concentration that reflects the prostate tumor growth

androgen dynamics, denoted by Σ_1 in Fig. 3, as follows:

$$\frac{\mathrm{d}a(t)}{\mathrm{d}t} = -\gamma\big(a(t) - a_0\big) - \gamma a_0 u(t), \tag{1}$$

where $a(t)$ (nmol/l) represents the serum androgen concentration, and $u(t) = 1$ for on-treatment periods and $u(t) = 0$ for off-treatment ones. The steady-state value of the normal androgen concentration is denoted by a_0 (nmol/l), which takes a value of $8 \le a_0 \le 35$ for usual adult males. The speed of the recovery and decay of the androgen concentration is governed by the exponent γ. Thus, (1) describes two different dynamics of the androgen level depending on the binary variable $u(t)$.

The tumor growth is described with changes in the populations of AD and AI cells. The proliferation and apoptosis rates of AD and AI cells are assumed to be dependent on the androgen concentration $a(t)$. Based on this setting, the tumor dynamics, denoted by Σ_2 in Fig. 3, is simply described as follows:

$$\frac{\mathrm{d}x_1(t)}{\mathrm{d}t} = \big\{\alpha_1 p_1\big(a(t)\big) - \beta_1 q_1\big(a(t)\big) - m\big(a(t)\big)\big\}x_1(t), \tag{2}$$

$$\frac{\mathrm{d}x_2(t)}{\mathrm{d}t} = m\big(a(t)\big)x_1(t) + \big\{\alpha_2 p_2\big(a(t)\big) - \beta_2 q_2\big(a(t)\big)\big\}x_2(t), \tag{3}$$

where $x_1(t)$ and $x_2(t)$ represent the populations of AD and AI cells, respectively. The coefficient of $x_1(t)$ in the right-hand side of (2) indicates the net growth rate of the AD cells, which is determined by the proliferation rate $\alpha_1 p_1$, the apoptosis rate $\beta_1 q_1$, and the mutation rate m by which AD cells mutate into AI cells. Similarly, in (3), $\alpha_2 p_2$ and $\beta_2 q_2$ represent the proliferation and the apoptosis rates of the AI cells, respectively. The coefficients α_1, β_1, α_2, and β_2 are the parameters that depend on the metastatic sites. The published data (Berges et al. 1995) on the daily percentages of cell proliferation and apoptosis are adopted to estimate the parameter values, as shown in Table 1. The values of α_1 and β_1 refer to the experimental data for hormonally untreated patients, while those of α_2 and β_2 refer to the data for hormonally failing patients. Since the corresponding parameter values under hormonal therapy are not available, we assume that the androgen-dependent functions can be described as follows (see also Jackson 2004a, 2004b):

$$p_1(a) = k_1 + (1 - k_1)\frac{a}{a + k_2}, \tag{4}$$

Table 1 Parameter values obtained from the experimental data (Berges et al. 1995)

Parameter	Bone metastasis	Lymph node metastasis
α_1 (days^{-1})	0.0204	0.0290
α_2 (days^{-1})	0.0242	0.0277
β_1 (days^{-1})	0.0076	0.0085
β_2 (days^{-1})	0.0168	0.0222

$$q_1(a) = k_3 + (1 - k_3)\frac{a}{a + k_4}, \tag{5}$$

$$p_2(a) = \begin{cases} \text{(i)} & 1, \\ \text{(ii)} & 1 - \left(1 - \frac{\beta_2}{\alpha_2}\right)\frac{a}{a_0}, \\ \text{(iii)} & 1 - \frac{a}{a_0}, \end{cases} \tag{6}$$

$$q_2(a) = 1, \tag{7}$$

$$m(a) = m_1\left(1 - \frac{a}{a_0}\right). \tag{8}$$

The biologically feasible values of the related parameters in these functions are discussed in Sect. 2.2.

We assume that the temporal variation of the serum PSA concentration $y(t)$ can be monitored as a biomarker for the prostate tumor growth (Swanson et al. 2001). Since a large amount of PSA is secreted by cancer cells, the PSA concentration is assumed to be represented by a linear function with the subpopulations of cancer cells as follows:

$$y(t) = c_1 x_1(t) + c_2 x_2(t). \tag{9}$$

The PSA concentration is the only observable output of the system as illustrated in Fig. 3 and used as a basis for the intermittent administration in the IAS therapy model.

2.2 Proliferation, Apoptosis, and Mutation Rates

The total tumor growth, determined by (2)–(3), is largely influenced by the functions (4)–(8). Figures 4 and 5 show how the proliferation, apoptosis, and mutation rates of the tumor cells in the model are dependent on the androgen concentration in the case of bone metastasis where $a_0 = 30$. We discuss the androgen dependence of the proliferation and apoptosis rates and estimation of the related parameters in the following.

Figure 4(a) shows the proliferation and apoptosis rates of the AD cells. Since the AD cells do not multiply without androgens, we set $k_1 = p_1(0) = 0$ in (4). The proliferation rate of the AD cells approximates α_1 under an androgen-rich environment because $p_1(a)$ approaches 1 with increasing a. We set $k_2 = 2$ in (4) to generate a plausible $\alpha_1 p_1(a)$ curve. On the other hand, the apoptosis rate of the AD cells ranges from β_1 in an androgen-rich state to $\beta_1 q_1(0) = \beta_1 k_3$ in an androgen-poor one. The value of $\beta_1 k_3$ can be estimated by fitting an exponential function to the decreasing

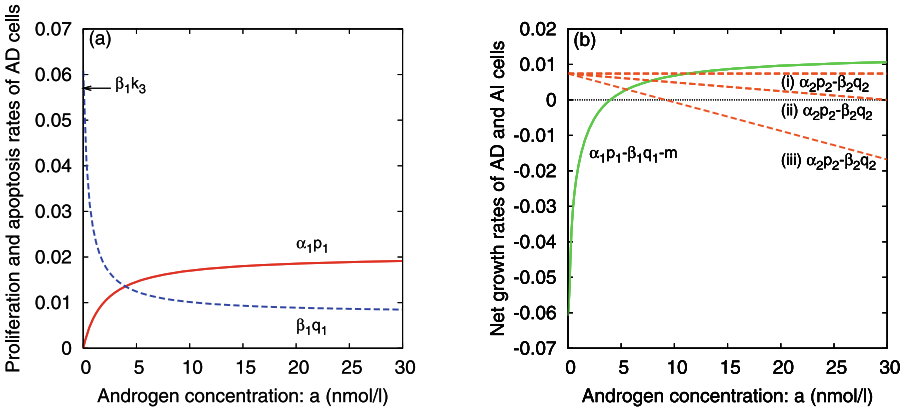

Fig. 4 (**a**) Androgen dependence of the proliferation and apoptosis rates of AD cells. (**b**) Androgen dependence of the net growth rates of the AD and AI cells

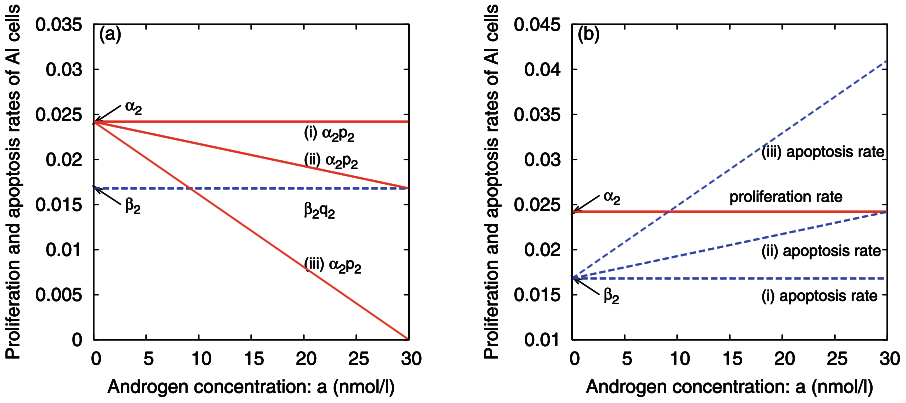

Fig. 5 Androgen dependence of the proliferation and apoptosis rates of AI cells. Three proliferation rate functions (i)–(iii) with a constant apoptosis rate in (**a**) and three apoptosis rate functions (i)–(iii) with a constant proliferation rate in (**b**) correspond to the same net growth rates (i)–(iii) of the AI cells in Fig. 4(**b**)

serum PSA concentration during the hormonal therapy. We obtained the approximate value $\beta_1 k_3 = 0.06$ from real PSA data (Bruchovsky et al. 2000, 2001, 2006, 2007), and set $k_3 = 8$ and $k_4 = 0.5$ in (5) so that the evolution of AD cells change from a decrease to an increase at about $a = 5$. Due to the relatively small mutation rate, the difference between the proliferation and the apoptosis rates approximates the net growth rate of the AD cells, as shown in Fig. 4(b). The curve of the net growth rate indicates that the population of the AD cells decreases by a greater rate for a lower androgen level.

The proliferation and apoptosis rates of the AI cells are also dependent on the androgen concentration (Kokontis et al. 1994) because their growth and apoptosis are still dependent on the androgen receptor (Dehm and Tindall 2005; Feldman and Feldman 2001; Scher et al. 2004; Edwards and Bartlett 2005), although details of

their androgen dependence remain unclear. Therefore, we first assume three possibilities on the net growth rate of the AI cells as shown in Fig. 4(b). For simplicity, we assume that the net growth rates are linear functions of a, even though in general they can be nonlinear functions (Kokontis et al. 1994). The three examples of the typical cases are shown in Fig. 4(b), which are characterized respectively by whether the net growth rate is positive, zero, or negative in an androgen-rich condition. The last assumption is adopted in the previous study (Jackson 2004a, 2004b) because the AI cells are usually below detectable levels before the initiation of the androgen suppression therapy. There exists biological evidence to support this assumption. Namely, it was shown experimentally with some kinds of AI cells (cell sublines of LNCaP 104-R1 and 104-R2 cells) that the proliferation of the AI cells is repressed by androgen and the net growth rates are negative in conditions with physiological concentrations of androgen (Kokontis et al. 1998, 2005; Chuu et al. 2005). Moreover, some experimental and clinical data of the PSA variations under the actual IAS therapy (Akakura et al. 1993; Bruchovsky et al. 2000, 2001) show that the levels of the PSA nadirs during the successive on-treatment periods are not necessarily increasing for several on-off cycles of the treatment. Since a population of the AI cells should increase in an androgen-poor condition as a cause of an AI relapse, these data also imply that the net growth rate of the AI cells may not be positive during the off-treatment periods; otherwise, the number of the AI cells should expand rapidly due to their always positive values of the net growth rate both during the on-treatment and during the off-treatment, resulting in a successive increase of the PSA nadir levels. Therefore, the latter two assumptions are also worth considering.

The three assumptions on the net growth rate of the AI cells correspond to the three proliferation rate functions with a constant apoptosis rate, respectively, as shown in Fig. 5(a). The three assumptions, which may result from properties of the AI cells (Kokontis et al. 1994, 1998, 2005; Chuu et al. 2005) as well as implicit competition with the AD cells (Shimada and Aihara 2007), can be described as follows.

(i) The proliferation rate of the AI cells remains constant, i.e., $\alpha_2 p_2(a_0) = \alpha_2$.
(ii) When the androgen level is normal, the population of the AI cells does not change, i.e., $\alpha_2 p_2(a_0) = \beta_2 < \alpha_2$.
(iii) When the androgen level is normal, the population of the AI cells decreases, i.e., $\alpha_2 p_2(a_0) = 0$.

The androgen-dependent functions defined in (6) correspond to the above three cases. Case (i) may be plausible. Cases (ii)–(iii) in (6) are also considered because androgenic repression of the AI cell proliferation is due in part to down-regulation of a proto-oncogene *c-myc*, and accumulation of the cell cycle inhibitor $p27^{Kip1}$, which in turn inhibits cyclin-dependent kinase 2 (Cdk2) and causes cell cycle G_1 arrest (Kokontis et al. 1998, 2005; Chuu et al. 2005). Figure 5(b) shows the equivalent counterpart of Fig. 5(a) in the sense that both yield the same net growth rates of AI cells in Fig. 4(b). Proliferation and apoptosis rates similar to Case (iii) in Fig. 5(b) were assumed in the previous study (Jackson 2004b). It should be noted that the functions of the proliferation and apoptosis rates (i), (ii), and (iii) in Fig. 5(a) and

those (i), (ii), and (iii) in Fig. 5(b) produce exactly the same dynamics because their differences representing the net growth rate of the AI cells are the same with functions (i), (ii), and (iii) in Fig. 4(b), respectively. Furthermore, any intermediate version of the proliferation and apoptosis rate functions of AI cells between Fig. 5(a) and (b), both of which are not constant, also generates the same dynamics if the difference or the net growth rate is the same. The signs of the net growth rates of the AD and AI cells are assumed not to be concurrently negative at any constant value of the androgen concentration in order to preclude trivial unrealistic cases in which the androgen level can be easily regulated so that the tumor undergoes regression consistently.

The maximum mutation rate m_1 significantly influences the time of a PSA relapse. As shown in Fig. 6, the development of the serum PSA concentration after the initiation of the medical castration sensitively depends on the value of m_1. The relapse time is not strictly defined, but an example of the practically used criterion for the PSA relapse, which should be distinguished from a clinical and symptomatic relapse, is a continuous increase in the serum PSA concentration more than 4 (ng/ml) with the serum testosterone less than 0.5 (nmol/l) in the three-time measurements with the inter-measurement interval of 4 weeks (Bruchovsky et al. 2000). The latency period until a relapse is usually around several years under CAS therapy. Based on these facts, Fig. 6 suggests a feasible range of the values of m_1. It should be noted that the mutation rate may actually depend on properties like the metastatic site and the grade of malignancy of the cancer cells.

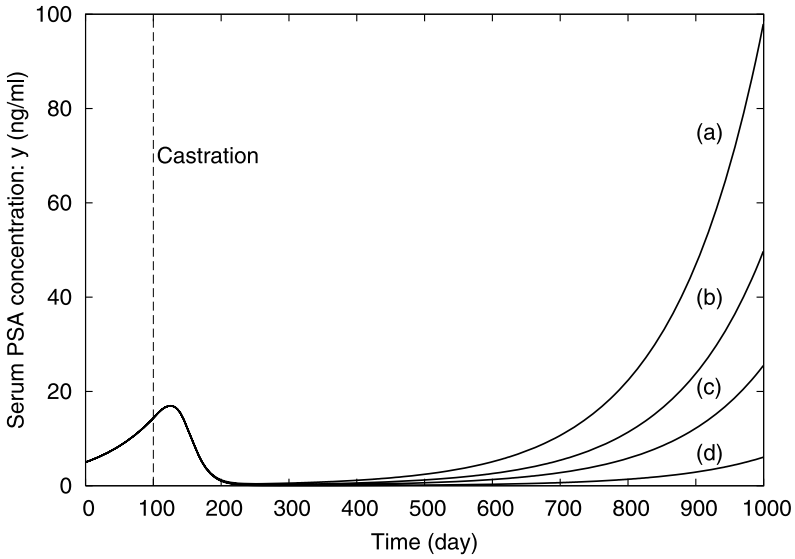

Fig. 6 Effect of the mutation rate on the relapse time under the CAS therapy in the case of bone metastasis. The temporal development of the serum PSA concentration y is computed by numerical simulations of (1)–(5), (6)(iii), and (7)–(9) with the following parameter values and initial conditions: $\gamma = 0.08$, $a_0 = 30$, $x_1(0) = 5$, $x_2(0) = 1$, $a(0) = 30$, and (**a**) $m_1 = 0.0002$, (**b**) $m_1 = 0.0001$, (**c**) $m_1 = 0.00005$, and (**d**) $m_1 = 0.00001$

3 Mathematical Model of Intermittent Androgen Suppression

A mathematical model of the IAS therapy is derived from the formulation in the previous section by introducing the intermittent administration, as shown in Fig. 7. As indicated by the hysteresis feedback loop in the block diagram, the administration is switched on and off with hysteresis, depending on the variation of the serum PSA concentration, which provides an indicator of the tumor growth. In other words, the administration is suspended when the serum PSA concentration falls below r_0 (ng/ml) during on-treatment periods and it is reinstituted when the concentration exceeds r_1 (ng/ml) during off-treatment periods. How to plan the IAS therapy or how to appropriately set the adjustable parameters, r_1 and r_0, under the condition of $r_1 > r_0 > 0$ (Bhandari et al. 2005) is a significant issue for clinical practice. A purpose of our modeling approach for IAS therapy is to obtain some suggestions on a protocol for the intermittent administration.

The complete model of the IAS therapy for prostate cancer is given as follows:

$$\frac{da(t)}{dt} = -\gamma\big(a(t) - a_0\big) - \gamma a_0 u(t), \tag{10}$$

$$\frac{dx_1(t)}{dt} = \big\{\alpha_1 p_1\big(a(t)\big) - \beta_1 q_1\big(a(t)\big) - m\big(a(t)\big)\big\}x_1(t), \tag{11}$$

$$\frac{dx_2(t)}{dt} = m\big(a(t)\big)x_1(t) + \big\{\alpha_2 p_2\big(a(t)\big) - \beta_2 q_2\big(a(t)\big)\big\}x_2(t), \tag{12}$$

$$y(t) = c_1 x_1(t) + c_2 x_2(t), \tag{13}$$

$$u(t) = \begin{cases} 0 \to 1 & \text{when} \quad y(t) = r_1 \quad \text{and} \quad dy(t)/dt > 0, \\ 1 \to 0 & \text{when} \quad y(t) = r_0 \quad \text{and} \quad dy(t)/dt < 0, \end{cases} \tag{14}$$

where the androgen-dependent functions $p_1(\cdot)$, $q_1(\cdot)$, $p_2(\cdot)$, $q_2(\cdot)$, and $m(\cdot)$ are given by (4)–(8). The dynamics of the tumor growth given by (11)–(12) is driven by the androgen dynamics in (10), which depends on the discrete variable u alternatively representing the presence or the absence of administration. Since the total model

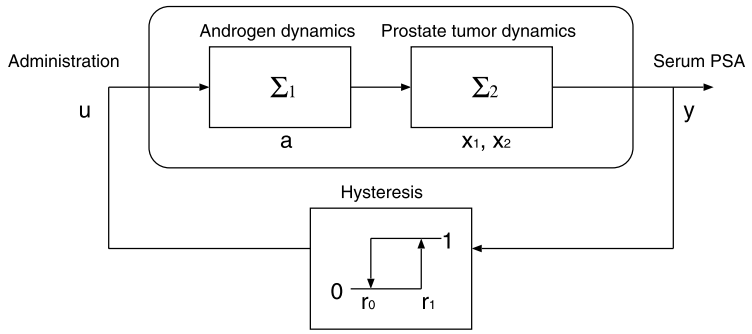

Fig. 7 Block diagram representing the IAS therapy. The administration is switched on and off with hysteresis in response to the temporal variation of the monitored serum PSA concentration

includes both continuous and discrete variables, it is called a hybrid dynamical system (Johnson 1994; Guckenheimer and Johnson 1995; van der Schaft and Schumacher 2000; Savkin and Evans 2001). The model dynamics is examined using numerical simulations and bifurcation analysis in the next two sections.

4 Numerical Simulations

The numerical simulations of the IAS therapy model (10)–(14) are first performed in order to investigate the difference among the three cases (i)–(iii) of the net growth rate of the AI cells in a prostate tumor. For each case, we consider the bone and lymph node metastases with the corresponding parameter values that are listed in Table 1. The exponent related to the increase and decrease of the androgen level, the steady-state value of the androgen concentration, and the maximum mutation rate are fixed at $\gamma = 0.08$, $a_0 = 30$, and $m_1 = 0.00005$, respectively. With regard to the administration, we examine how the PSA level r_0, which discontinues the androgen deprivation, influences the relapse time when $r_1 = 15$. This value of r_1 is determined from the clinical study (Goldenberg et al. 1995) in which the androgen suppression is suspended until the serum PSA level increases up to a mean value between 10 (ng/ml) and 20 (ng/ml). The value of r_0 is required to be positive and less than r_1 for the IAS therapy. The model can be viewed to describe the CAS therapy if $r_0 = 0$. In addition, it is assumed that the AD and AI cells equivalently secrete PSA, i.e., $c_1 = c_2 = 1$. In our simulation study, divergent and nondivergent solutions are regarded to signify the occurrence and the prevention of a relapse, respectively.

Figures 8(a)–(b) show the time evolutions of the serum PSA concentration $y(t)$ in case (i), where the solid and dashed lines correspond to CAS and IAS, respectively.

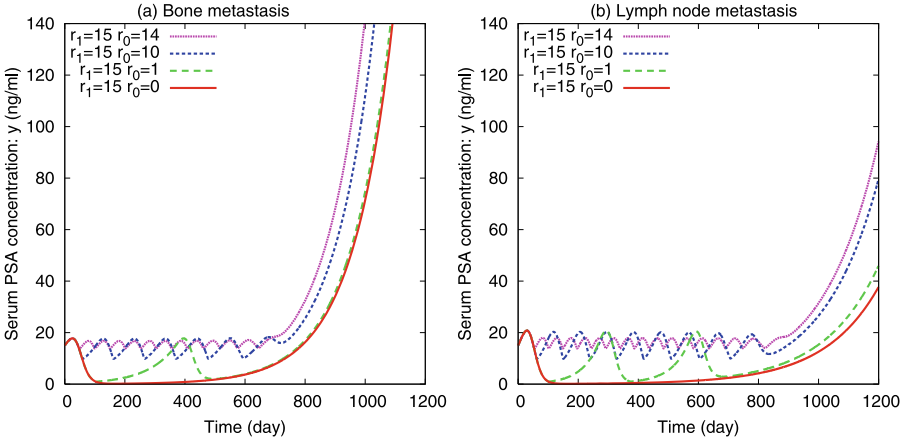

Fig. 8 (Color online) Time evolutions of the serum PSA concentration $y(t)$ in case (i), which are computed by the numerical simulations of (10)–(14) with the following parameter values and initial conditions: $\gamma = 0.08$, $a_0 = 30$, $m_1 = 0.00005$, $r_1 = 15$, $x_1(0) = 15$, $x_2(0) = 0.1$, $a(0) = 30$, and $u(0) = 1$. The *solid line* corresponds to the CAS therapy with $r_0 = 0$, while the *dashed lines* indicate the IAS therapy with different values of r_0. (**a**) Bone metastasis. (**b**) Lymph node metastasis

In Fig. 8(a), IAS seems to be more ineffective than CAS in postponing a relapse. However, a relapse occurs within approximately 3 years in all the trials with different values of r_0. Therefore, the IAS therapy is worthwhile in the sense that the periods of off-treatment introduced by this therapy can redress adverse effects of androgen deprivation. When the IAS therapy is adopted, the PSA level oscillates until a relapse takes place. Since r_0 influences the PSA nadir, a low level of r_0 enables to avoid too frequently repeated switching between the on-treatment and the off-treatment with short intervals. The qualitative property of the tumor growth in the lymph node metastasis is similar to that in the bone metastasis, as shown in Fig. 8(b). During the off-treatment periods, the tumor grows more rapidly in the lymph node metastasis due to the larger growth rate of the AD cells. However, the relapse is more delayed in the case of the lymph node metastasis because the net growth rate of the AI cells, which is responsible for the relapse, is less than that in the bone metastasis. The result, assuming that the net growth rate of the AI cells is constant, suggests that IAS may not improve the clinical efficacy of CAS in the relapse time but it could be potentially useful in practical application in terms of the reduction in side effects.

The development of the serum PSA concentration $y(t)$ in case (ii) is depicted in Figs. 9(a)–(b). Unlike the previous case, all the trials with the IAS therapy remarkably extend the relapse time when compared with the CAS therapy. In particular, by setting r_0 to a marginal value, the IAS therapy can delay the relapse time by approximately more than a year. This is because the PSA nadir strongly influences the relapse time as the initial condition for the eventual exponential AI relapse. It is, however, impossible to avoid an eventual relapse in this case. The result, assuming that the population of the AI cells remains constant in an androgen-rich environment, suggests that IAS substantially contributes to retarding the progression to a fatal AI state.

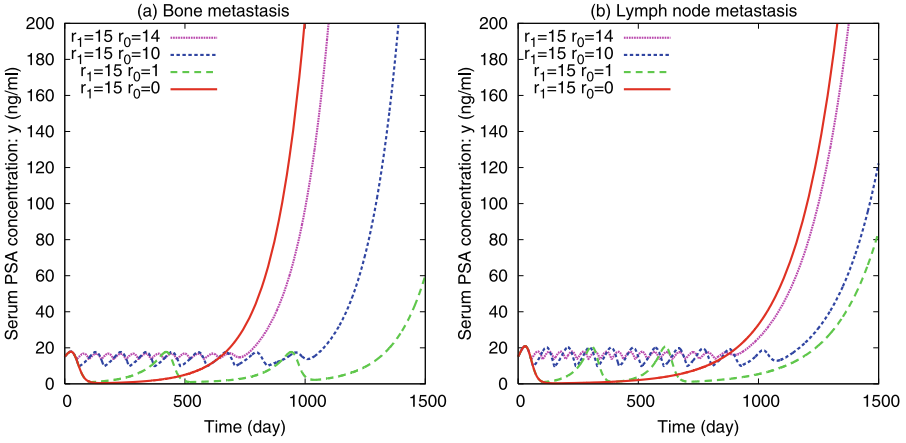

Fig. 9 (Color online) Time evolutions of the serum PSA concentration $y(t)$ in case (ii), which are computed by the numerical simulations of (10)–(14) with the following parameter values and initial conditions: $\gamma = 0.08$, $a_0 = 30$, $m_1 = 0.00005$, $r_1 = 15$, $x_1(0) = 15$, $x_2(0) = 0.1$, $a(0) = 30$, and $u(0) = 1$. The *solid line* indicates the CAS therapy with $r_0 = 0$, while the *dashed lines* indicate the IAS therapy with different values of r_0. (**a**) Bone metastasis. (**b**) Lymph node metastasis

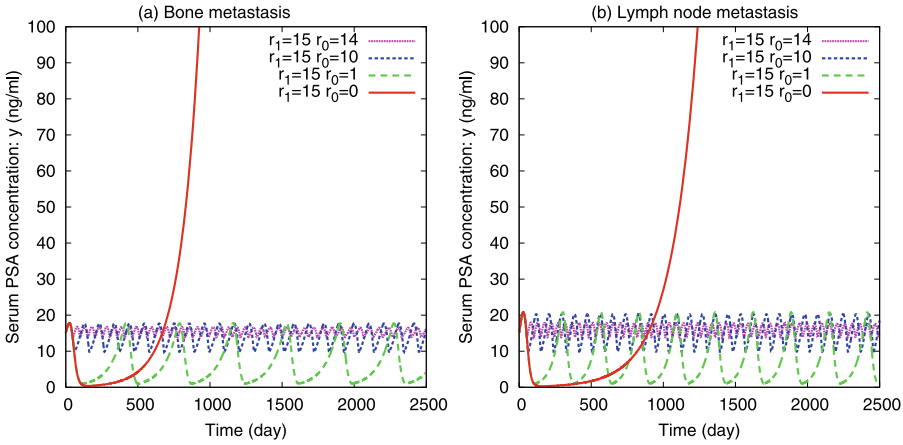

Fig. 10 (Color online) Time evolutions of the serum PSA concentration $y(t)$ in case (iii), which are computed by the numerical simulations of (10)–(14) with the following parameter values and initial conditions: $\gamma = 0.08$, $a_0 = 30$, $m_1 = 0.00005$, $r_1 = 15$, $x_1(0) = 15$, $x_2(0) = 0.1$, $a(0) = 30$, and $u(0) = 1$. The *solid line* indicates the CAS therapy with $r_0 = 0$, while the *dashed lines* indicate the IAS therapy with different values of r_0. (**a**) Bone metastasis. (**b**) Lymph node metastasis

Figures 10(a)–(b) show the temporal variations of the serum PSA concentration $y(t)$ in case (iii). The development of the PSA level under CAS is almost the same as those in cases (i) and (ii), due to the common net growth rate of AI cells in an androgen-deprived state. We can observe that CAS leads to a relapse within approximately 3 years, while IAS leads to repetitive growth and regression of the tumor without a relapse. As in the previous two cases, a smaller value of r_0 is desirable for reducing the frequency of the on-off cycles of administration. Figure 11 shows an example of the cycles of the androgen concentration and the serum PSA concentration under successful IAS therapy. The androgen concentration switches its dynamics at the instants of suspension and reinstitution of administration. On the other hand, there is a time lag between the reinstitution of administration and a decrease in the PSA level. This can be interpreted as an expression of the time latency required for a tumor to react to androgen deprivation. The result, assuming that the population of the AI cells decreases in an androgen-rich environment, suggests that IAS is much more effective than CAS in dealing with an AI relapse.

5 Bifurcation Analysis

It has been shown in the previous section that the IAS therapy enables to avoid a relapse only in case (iii). Whether a relapse occurs or not can be determined by the asymptotic behavior of the solution in the IAS therapy model. If a relapse is averted successfully, the solution typically converges to a stable limit cycle. The parameter region in which a relapse takes place can be characterized by the divergence of the solution. In this section, we further investigate how the net growth rate of the AI cells and the PSA-based administration affect the resulting solutions under CAS and IAS.

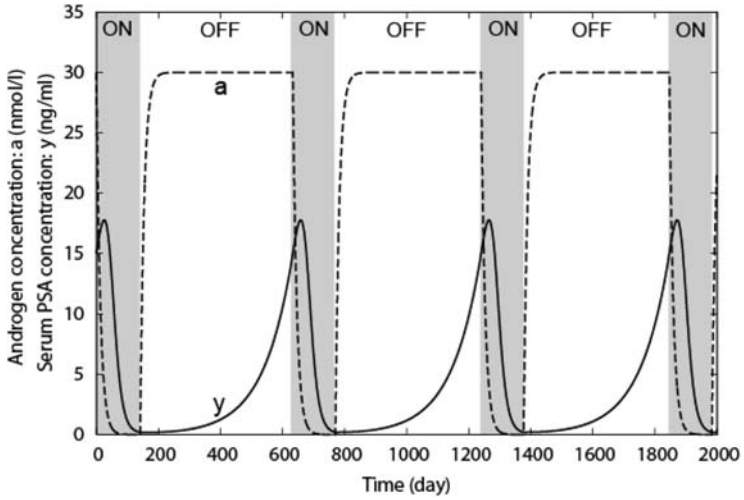

Fig. 11 Cycles of the serum PSA concentration $y(t)$ and the androgen concentration $a(t)$ under successful IAS therapy in case (iii). The time courses are computed by numerical simulations of (10)–(14) with the following parameter values and initial conditions: $\gamma = 0.08$, $a_0 = 30$, $m_1 = 0.00005$, $r_1 = 15$, $r_0 = 0.2$, $x_1(0) = 15$, $x_2(0) = 0.01$, $a(0) = 30$, and $u(0) = 1$

The proliferation rate of the AI cells given in (6) can be continuously parameterized beyond cases (i), (ii), and (iii), using parameter d as follows:

$$p_2(a) = 1 - da/a_0, \tag{15}$$

where $d = 0$ for case (i), $d = 1 - \beta_2/\alpha_2$ for case (ii), and $d = 1$ for case (iii). Hence, the androgen dependence of the net growth rate of the AI cells, as shown in Fig. 4(b), can be continuously adjusted by parameter d in the range of $0 \le d \le 1$.

Figures 12(a)–(b) show the phase diagrams that demonstrate how the behavior of the orbit after the transient period is affected by the PSA level r_0 to discontinue androgen deprivation and parameter d. The gray region indicates the parameter condition with which the prostate tumor growth can be successfully prevented using the intermittent administration. In the white region, a relapse eventually occurs with an explosion in both the population of the AI cells and the PSA concentration. It is feasible that a relapse cannot be avoided if the value of d is smaller than that in case (ii) because the growth rate of the AI cells is positive regardless of the androgen level, as shown in Fig. 4(b). In other words, an AI relapse is inevitable in this model unless the proliferation rate of AI cells takes a negative value for a certain range of the androgen concentration. The solid curves indicating the period-doubling bifurcations of a stable limit cycle are along the boundary between the two regions with qualitatively different solutions. They are obtained by tracing the bifurcation points using a shooting method (Kousaka et al. 1999). In addition to a one-folded limit cycle, multiple-folded limit cycles and even chaotic solutions can be found near the boundary. These solutions are also considered to signify relapse prevention because they are confined in a finite region in the phase space. Figure 13 shows examples of the orbital motions and the corresponding PSA variations. Figure 13(a) corresponds to the CAS

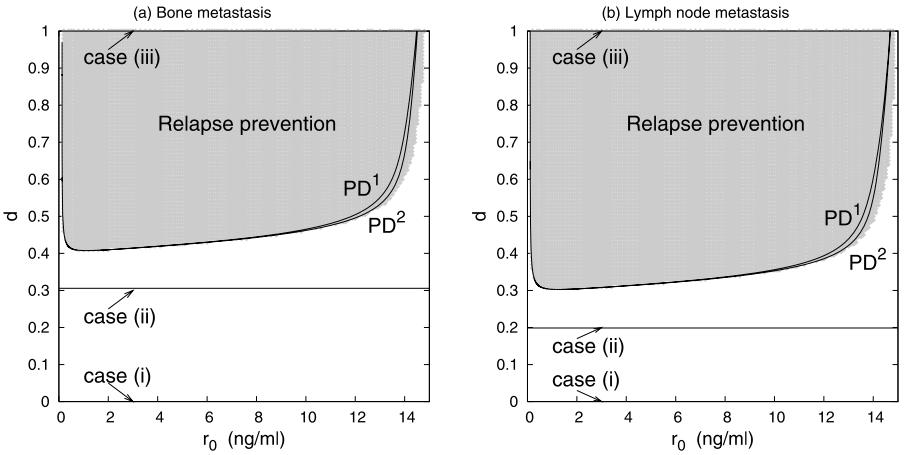

Fig. 12 Phase diagrams showing the regions of a relapse (*white*) and relapse prevention (*gray*), which are computed by the numerical simulations of (10)–(15) using the following parameter values: $\gamma = 0.08$, $a_0 = 30$, $m_1 = 0.00005$, and $r_1 = 15$. The *solid curve* denoted by PD^m ($m = 1, 2$) indicates the period-doubling bifurcation of an m-folded limit cycle. (**a**) Bone metastasis. (**b**) Lymph node metastasis

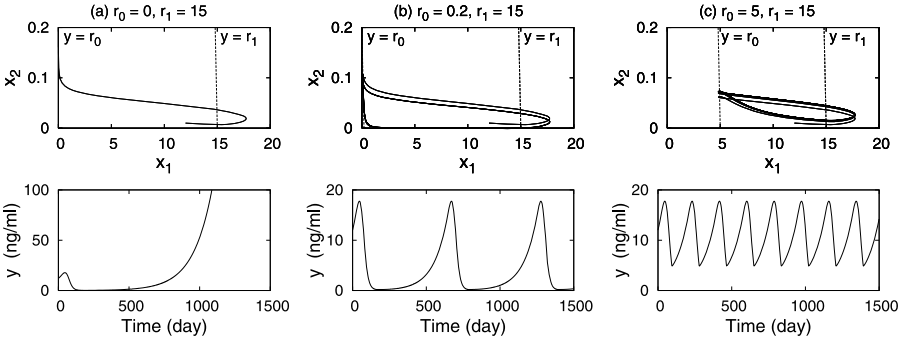

Fig. 13 Orbital motions (*upper*) and time series of the PSA concentration (*lower*), which are computed by the numerical simulations of (10)–(15) using the following parameter values and initial conditions: $\gamma = 0.08$, $a_0 = 30$, $m_1 = 0.00005$, $d = 1$, $x_1(0) = 12$, $x_2(0) = 0.01$, $a(0) = 30$, and $u(0) = 0$. (**a**) $(r_0, r_1) = (0, 15)$. (**b**) $(r_0, r_1) = (0.2, 15)$. (**c**) $(r_0, r_1) = (5, 15)$

therapy with $r_0 = 0$, at which the AD cell population almost vanishes but the AI cell population increases to infinity. If r_0 is not too small, the orbit can intersect with the dashed line corresponding to the criterion for the suspension of administration and thereby exhibit periodic motions, as shown in Fig. 13(b). The intersection is maintained with the increase in r_0, as shown in Fig. 13(c), although there is an increase in the frequency of the on-off cycles of administration.

Figures 14(a)–(b) show similar bifurcation diagrams where the horizontal axis represents the PSA level r_1 to reinstitute administration. In these diagrams, r_0 is fixed at a sufficiently small value, assuming that the administration may be suspended if androgen is almost completely deprived by medical castration. A relapse can be prevented if the net growth rate of the AI cells takes negative values for some range of

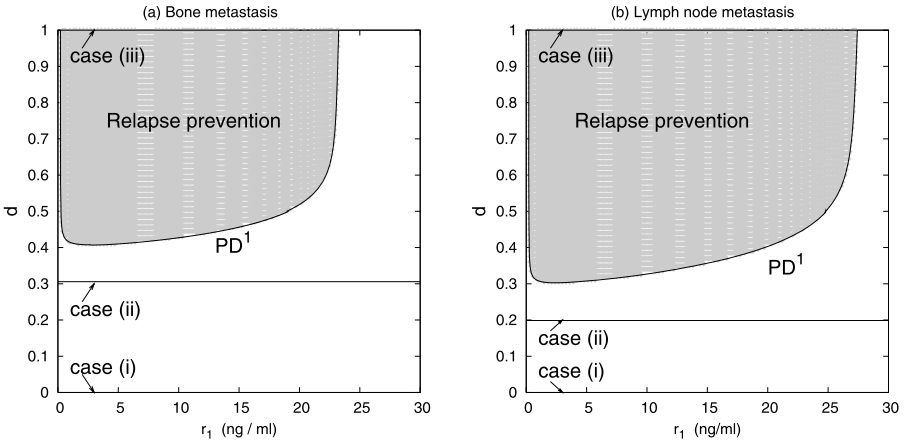

Fig. 14 Phase diagrams showing the regions of a relapse (*white*) and relapse prevention (*gray*), which are computed by the numerical simulations of (10)–(15) using the following parameter values: $\gamma = 0.08$, $a_0 = 30$, $m_1 = 0.00005$, and $r_0 = 0.2$. The *solid curve* denoted by PD^1 indicates a set of period-doubling bifurcations of a limit cycle. (**a**) Bone metastasis. (**b**) Lymph node metastasis

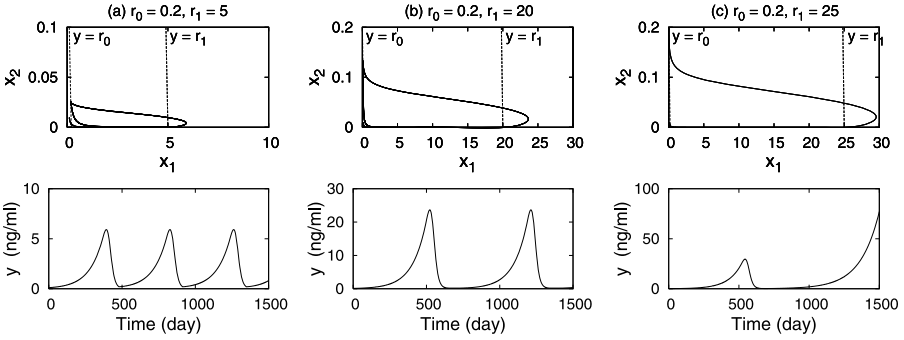

Fig. 15 Orbital motions (*upper*) and time series of the PSA concentration (*lower*), which are computed by the numerical simulations of (10)–(15) using the following parameter values and initial conditions: $\gamma = 0.08$, $a_0 = 30$, $m_1 = 0.00005$, $d = 1$, $x_1(0) = 0.1$, $x_2(0) = 0.01$, $a(0) = 30$, and $u(0) = 0$. (**a**) $(r_0, r_1) = (0.2, 5)$. (**b**) $(r_0, r_1) = (0.2, 20)$. (**c**) $(r_0, r_1) = (0.2, 25)$

the androgen concentration and r_1 is not too large. The range of r_1 to avoid a relapse is more restricted in the case of bone metastasis than in lymph node metastasis because of the difference in the growth rates of the AD and AI cells. The qualitative change in the solutions with an increase in r_1 is shown in Fig. 15. Figures 15(a)–(b) demonstrate that the maximum value of the PSA concentration is controlled by r_1 if the tumor growth exhibits a repetitive cycle. For a very large value of r_1, however, the orbit fails to meet the criterion for the suspension of administration and escapes to the infinity along the x_2 axis, as shown in Fig. 15(c).

Next, the effect of the mutation rate on a relapse under the IAS therapy is examined in Figs. 16(a)–(b). The relapse can be prevented in the case with a relatively

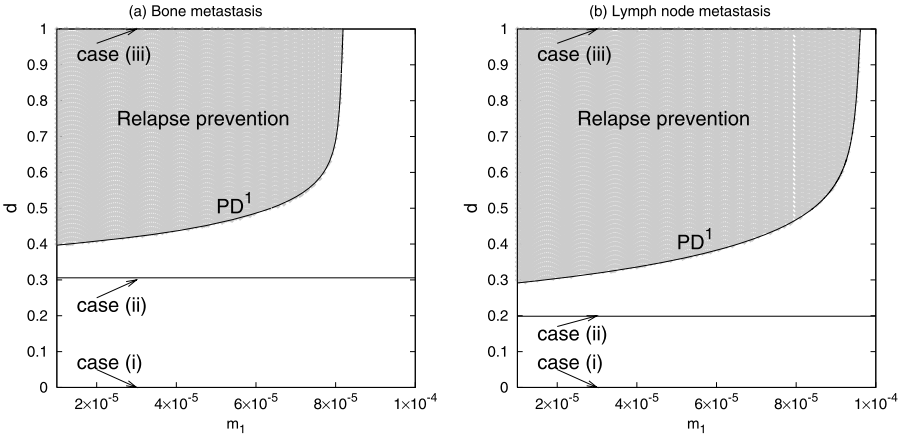

Fig. 16 Phase diagrams showing the regions of a relapse (*white*) and relapse prevention (*gray*), which are computed by the numerical simulations of (10)–(15) using the following parameter values: $\gamma = 0.08$, $a_0 = 30$, $m_1 = 0.00005$, $r_0 = 0.2$, and $r_1 = 15$. The *solid curve* denoted by PD^1 indicates a set of period-doubling bifurcations of a limit cycle. (**a**) Bone metastasis. (**b**) Lymph node metastasis

small value of the maximum mutation rate in both the metastases. An increase in the maximum mutation rate facilitates the population growth of the AI cells during an on-off cycle of administration. Therefore, if the value of m_1 is large enough, an orbit under on-treatment cannot reach the plane $y = r_0$ corresponding to the condition for the suspension of administration.

The parameter conditions for relapse prevention, which have been revealed by the bifurcation analysis, suggest that both r_1 and r_0 are jointly responsible for the efficacy of the IAS therapy. A small positive value of r_0 is desirable for holding down the PSA nadir and delaying a relapse; however, the value should not be too small because IAS will otherwise result in CAS without discontinuing the administration. The value of r_1 should not be very large in order to reduce the risk of an AI relapse resulting from the increase in the population of the AI cells during the on-treatment periods. In clinical practice, the frequency of the on-off cycles of administration is dependent on patient characteristics like the baseline and nadir levels of the serum PSA (Bruchovsky et al. 2006, 2007). For example, according to the data of the Canadian prospective phase II trials of IAS (Bruchovsky et al. 2006), mean times of on-treatment and off-treatment are 29.6–34.5 weeks and 25.6–63.7 weeks, respectively. Figure 15 suggests that the frequency of administration in the IAS therapy model is realistic if r_0 is set at a small value. These results obtained by the mathematical modeling suggest that the IAS therapy can be useful at least for delaying the relapse time even if a relapse eventually occurs.

6 Discussion

A number of experimental and clinical studies on prostate cancer therapy have confirmed that CAS therapy as a normal treatment for advanced prostate cancer often

results in recurrent tumor growth despite its beneficial short-term effect. A mathematical model describing an AI relapse under ADT and MAB was presented by Jackson (2004a, 2004b) in the form of partial differential equations. The model reproduced well the recurrent tumor growth during the CAS therapy by describing the tumor as a mixed group of AD and AI cells, and its analysis provided a condition for an AI relapse. Based on formulation similar to the previous model, we have proposed a mathematical model representing tumor growth under IAS therapy, whose actual effect is currently being evaluated through the phase II and the ongoing phase III trials (Bhandari et al. 2005; Bruchovsky et al. 2006, 2007). In addition to the cellular proliferation and apoptosis driven by androgens, the proposed model has taken into consideration the mutational effect especially in an androgen-deprived state. Intermittent administration performed with the monitoring of the serum PSA concentration has been modeled by a hysteretic feedback loop, resulting in a hybrid dynamical system where a discrete variable alternatively representing the presence or the absence of administration works as a control variable. The issue of how to optimally plan the intermittent treatment for relapse prevention has been reduced to the problem of how to appropriately choose the criteria for switching the control variable in the mathematical model.

Although the AI cells are assumed to be responsible for the prostate cancer relapse, how the androgen influences on AI cell growth is still not fully understood in spite of many experimental studies (Feldman and Feldman 2001; McLeod 2003; Scher et al. 2004; Dehm and Tindall 2005; Edwards and Bartlett 2005; Kokontis et al. 1994, 1998). Thus, we have first simulated the IAS therapy model under three possible hypotheses on the net growth rate of AI cells, and next analyzed the bifurcation structure by changing a parameter of the AI growth rate continuously as a bifurcation parameter. Under the hypothesis that the population of AI cells decreases in an androgen-rich condition, a relapse can be avoided depending on the manner of intermittent administration and on patient's characteristics. The important problem concerning the numerical results is how to appropriately determine the switching PSA levels in order to suspend and reinstitute administration in a clinically feasible range. It should be noted that a relapse is inevitable in our model regardless of the protocol of intermittent administration if the net growth rate of AI cells is positive for any androgen level like in case (i). However, if we introduce competition, e.g., for nutrition, between AD cells and AI ones into the model, it is possible to prevent a relapse even in case (i) (Shimada and Aihara 2007). This kind of modification of the model is an important future problem.

The bifurcation analysis has revealed parameter regions for relapse prevention which is characterized by a nondivergent solution. A typical example of such a solution is a stable limit cycle in the state space. The observation of the orbital motions has shown that a solution diverges with $x_2 \to \infty$ if an orbit in the on-treatment periods fails to attain the criterion for the suspension of administration. In this criterion, there is a trade-off between reducing the risk of a relapse and reducing the frequency of the on-off cycles of administration. Moreover, the administration should be reinstituted at an appropriate PSA level in order to prevent on-treatment periods from becoming very long. Otherwise, the development of the AI cells during a long on-treatment period would enhance the risk of a relapse. The numerical results have indicated the

importance of appropriately setting together the two adjustable parameters r_0 and r_1 of the intermittent administration.

The bifurcation analysis has focused on the qualitative difference in attractors, i.e., the asymptotic states of the solution. It has enabled to separate the regimes of prevention and occurrence of a relapse in the parameter space. However, in clinical practice, even if a relapse cannot be avoided, it is essentially important to prolong a relapse as long as possible. With respect to this point, a possible strategy is to confine a long-term transient orbit in a bounded region by adopting more flexible feedback control. Further, it is necessary to examine the effects of the parameters whose values are fixed in the numerical simulations. In particular, the steady-state value of the androgen concentration is likely to be closely related to tumor growth and the frequency of on-off cycles of administration.

Our model of the IAS therapy for prostate cancer has provided an insight into the optimal intermittent administration to prevent an AI relapse. The results have shown a possibility that the IAS therapy with an appropriately designed protocol of treatment can be better than the CAS therapy in terms of clinical efficacy such as reduction in medical expenses, alleviation of side effects and improvement in the quality of life during the off-treatment periods, and possible delay or prevention of a relapse under the hypothesis on the net growth rates of the AI cells like case (iii). It should be noted that the hypothesis needs further medical and biological verification, e.g., by using radical prostatectomy specimens from patients and their primary cultures (Berges et al. 1995) toward more realistic modeling, although there is biological evidence that the net growth rates of AI cells are negative in conditions with physiological concentrations of androgen (Kokontis et al. 1998, 2005; Chuu et al. 2005) as explained in Sect. 2.2.

The clinical data during the IAS therapy have shown a variety of patients' response patterns (Bruchovsky et al. 2000, 2001, 2006, 2007; Bhandari et al. 2005). Then it seems necessary to consider individuality of each patient for modeling. As an example of such individuality, we have changed the parameter d of the net growth rate of AI cells as the bifurcation parameter. It is an important future problem to validate or invalidate our model with real clinical data. A possible methodology for this evaluation is to fit our model to real data and check its predictability (Sauer et al. 1991; Ott et al. 1994; Weigend and Gershenfeld 1994; Abarbanel 1996; Kantz and Schreiber 1997) with respect to temporal evolution of the serum PSA time series data. The study for this direction with data of the Canadian prospective phase II trial (Bruchovsky et al. 2006, 2007) is now ongoing to be published elsewhere. Such modeling with clinical data may realize tailor-made IAS therapy for each patient in future. This kind of collaboration between theory and real data should be indispensable for development of a useful model of prostate cancer and its clinical application (Byrne et al. 2006).

Acknowledgements The authors would like to thank Prof. P. Holmes of Princeton University, Prof. N. Bruchovsky of the Prostate Centre at Vancouver General Hospital, University of British Columbia, and Dr. T. Shimada of the Graduate School of Engineering, University of Tokyo, for their valuable comments.

References

Abarbanel, H.D.I.: Analysis of Observed Chaotic Data. Springer, New York (1996)

Akakura, K., Bruchovsky, N., Goldenberg, S.L., Rennie, P.S., Buckley, A.R., Sullivan, L.D.: Effects of intermittent androgen suppression on androgen-dependent tumors: Apoptosis and serum prostate-specific antigen. Cancer **71**(9), 2782–2790 (1993)

Berges, R.R., Vukanovic, J., Epstein, J.I., CarMichel, M., Cisek, L., Johnson, D.E., Veltri, R.W., Walsh, P.C., Isaacs, J.T.: Implication of cell kinetic changes during the progression of human prostatic cancer. Clin. Cancer Res. **1**, 473–480 (1995)

Bhandari, M.S., Crook, J., Hussain, M.: Should intermittent androgen deprivation be used in routine clinical practice? J. Clin. Oncol. **23**(32), 8212–8218 (2005)

Bladou, F., Vessella, R.L., Buhler, K.R., Ellis, W.J., True, L.D., Lange, P.H.: Cell proliferation and apoptosis during prostatic tumor xenograft involution and regrowth after castration. Int. J. Cancer **67**, 785–790 (1996)

Bruchovsky, N., Rennie, P.S., Coldman, A.J., Goldenberg, S.L., To, M., Lawson, D.: Effects of androgen withdrawal on the stem cell composition of the Shionogi carcinoma. Cancer Res. **50**(8), 2275–2282 (1990)

Bruchovsky, N., Snoek, R., Rennie, P.S., Akakura, K., Goldenberg, S.L., Gleave, M.: Control of tumor progression by maintenance of apoptosis. Prostate Suppl. **6**, 13–21 (1996)

Bruchovsky, N., Klotz, L.H., Sadar, M., Crook, J.M., Hoffart, D., Godwin, L., Warkentin, M., Gleave, M.E., Goldenberg, S.L.: Intermittent androgen suppression for prostate cancer: Canadian prospective trial and related observations. Mol. Urol. **4**(3), 191–199 (2000)

Bruchovsky, N., Goldenberg, S.L., Mawji, N.R., Sadar, M.D.: Evolving aspects of intermittent androgen blockade for prostate cancer: diagnosis and treatment of early tumor progression and maintenance of remission. In: Andrology in the 21st Century. Proceedings of the VIIth International Congress of Andrology, pp. 609–623 (2001)

Bruchovsky, N., Klotz, L., Crook, J., Malone, S., Ludgate, C., Morris, W.J., Gleave, M.E., Goldenberg, S.L.: Final results of the Canadian prospective phase II trial of intermittent androgen suppression for men in biochemical recurrence after radiotherapy for locally advanced prostate cancer: Clinical parameters. Cancer **107**(2), 389–395 (2006)

Bruchovsky, N., Klotz, L., Crook, J., Larry, S., Goldenberg, S.L.: Locally advanced prostate cancer—Biochemical results from a prospective phase II study of intermittent androgen suppression for men with evidence of prostate-specific antigen recurrence after radiotherapy. Cancer **109**(5), 858–867 (2007)

Byrne, H.M., Alarcon, T., Owen, M.R., Webb, S.D., Maini, P.K.: Modelling aspects of cancer dynamics: A review. Phil. Trans. R. Soc. A **364**, 1563–1578 (2006)

Chuu, C., Hiipakka, R.A., Fukuchi, J., Kokontis, J.M., Liao, S.: Androgen causes growth suppression and reversion of androgen-independent prostate cancer xenografts to an androgen-stimulated phenotype in athymic mice. Cancer Res. **65**(6), 2082–2084 (2005)

Dehm, S.M., Tindall, D.J.: Regulation of androgen receptor signaling in prostate cancer. Expert Rev. Anticancer Ther. **5**(1), 63–74 (2005)

Edwards, J., Bartlett, J.M.S.: The androgen receptor and signal-transduction pathways in hormone-refractory prostate cancer. Part 1: Modifications to the androgen receptor. BJU Int. **95**, 1320–1326 (2005)

Feldman, B.J., Feldman, D.: The development of androgen-independent prostate cancer. Nat. Rev. Cancer **1**, 34–45 (2001)

Goldenberg, S.L., Bruchovsky, N., Gleave, M.E., Sullivan, L.D., Akakura, K.: Intermittent androgen suppression in the treatment of prostate cancer: A preliminary report. Urology **45**, 839–844 (1995)

Guckenheimer, J., Johnson, S.: Planar hybrid systems. In: Hybrid Systems II. Lecture Notes in Computer Science, vol. 999, pp. 202–225. Springer, Berlin (1995)

Huggins, C., Hodges, C.V.: Studies on prostatic cancer: I. The effect of castration, of estrogen and of androgen injection on serum phosphatases in metastatic carcinoma of the prostate. Cancer Res. **1**, 293–297 (1941)

Jackson, T.L.: A mathematical model of prostate tumor growth and androgen-independent relapse. Discrete Cont. Dyn. Syst. Ser. B **4**(1), 187–201 (2004a)

Jackson, T.L.: A mathematical investigation of the multiple pathways to recurrent prostate cancer: Comparision with experimental data. Neoplasia **6**(6), 697–704 (2004b)

Johnson, S.D.: Simple hybrid systems. Int. J. Bifurcat. Chaos **4**(6), 1655–1665 (1994)

Kantz, H., Schreiber, T.: Nonlinear Time Series Analysis. Cambridge University Press, Cambridge (1997)
Kokontis, J., Takakura, K., Hay, N., Liao, S.: Increased androgen receptor activity and altered *c-myc* expression in prostate cancer cells after long-term androgen deprivation. Cancer Res. **54**, 1566–1573 (1994)
Kokontis, J., Hay, N., Liao, S.: Progression of LNCaP prostate tumor cells during androgen deprivation: Hormone-independent growth, repression of proliferation by androgen, and role for $p27^{Kip1}$ in androgen-induced cell cycle arrest. Mol. Endocrinol. **12**(7), 941–953 (1998)
Kokontis, J., Hsu, S., Chuu, C., Dang, M., Fukuchi, J., Hiipakka, R.A., Liao, S.: Role of androgen receptor in the progression of human prostate tumor cells to androgen independence and insensitivity. Prostate **65**(4), 287–298 (2005)
Kousaka, T., Ueta, T., Kawakami, H.: Bifurcation of switched nonlinear dynamical systems. IEEE Trans. Circ. Syst. II **46**(7), 878–885 (1999)
McLeod, D.G.: Hormonal therapy: Historical perspective to future directions. Urology **61**, 3–7 (2003)
Nelson, W.G., De Marzo, A.M., Isaacs, W.B.: Mechanisms of disease: Prostate cancer. N. Engl. J. Med. **349**, 366–381 (2003)
Ott, E., Sauer, T., Yorke, J.A. (eds.): Coping with Chaos. Wiley, New York (1994)
Sauer, T., Yorke, J.A., Casdagli, M.: Embedology. J. Stat. Phys. **65**(3/4), 579–616 (1991)
Savkin, A.V., Evans, R.J.: Hybrid Dynamical Systems: Controller and Sensor Switching Problems. Springer, Berlin (2001)
Scher, H.I., Buchanan, G., Gerald, W., Butler, L.M., Tilley, W.D.: Targeting the androgen receptor: improving outcomes for castration-resistant prostate cancer. Endocr.-Relat. Cancer **11**, 459–476 (2004)
Shimada, T., Aihara, K.: A nonlinear model with competition between tumor cells and its application to intermittent androgen suppression therapy of prostate cancer. Tech. rep., Department of Mathematical Informatics, Graduate School of Information Science and Technology, University of Tokyo, METR 2007-10, Feb. (2007)
Swanson, K.R., True, L.D., Lin, D.W., Buhler, K.R., Vessella, R., Murray, J.D.: A quantitative model for the dynamics of serum prostate-specific antigen as a marker for cancerous growth: An explanation for a medical anomaly. Am. J. Pathol. **158**(6), 2195–2199 (2001)
van der Schaft, A.J., Schumacher, J.M.: An Introduction to Hybrid Dynamical Systems. Lecture Notes in Control and Information Sciences, vol. 251. Springer, Berlin (2000)
Weigend, A.S., Gershenfeld, N.A. (eds.): Time Series Prediction: Forecasting the Future and Understanding the Past. Addison-Wesley, Reading (1994)